Laser induced reactions in a 22-pole ion trap: $C_2H_2^+ + h\nu_3 + H_2 \rightarrow C_2H_3^+ + H$

Stephan Schlemmer, Emmanuelle Lescop, Jan von Richthofen, and Dieter Gerlich
Institute of Physics, University of Technology, D-09107 Chemnitz, Germany

Mark A. Smith
Department of Chemistry, University of Arizona, Tucson, Arizona 85721

(Received 13 March 2002; accepted 30 April 2002)

A sensitive experimental method for ion spectroscopy and state specific reaction dynamics is described, briefly called laser induced reactions (LIR). The technique is based on (i) trapping ions over a long time in a cold 22-pole rf ion trap followed by mass spectrometric detection, (ii) providing a suitable low density gas environment for collisions, (iii) modifying the low temperature chemical kinetics using selective excitation via a tunable radiation source. In this paper, the H-atom transfer reaction $C_2H_2^+ (v_3=1,J) + H_2 \rightarrow C_2H_3^+ + H$, is used to monitor the infrared excitation of acetylene ions. Rotationally resolved spectra are presented for the antisymmetric C–H stretching vibration. For recording a spectrum, it is sufficient to fill the trap with a few thousand parent ions. Differences with respect to conventional IR spectroscopy are discussed, especially the processes which influence the LIR signal. From the measured intensities and their dependence on parameters such as storage time, laser fluence and target gas density, information on state specific rate coefficients has been obtained at an ambient temperature of 90 K. Based on a model simulating the kinetics, rate coefficients for various inelastic and reactive collisions are derived. Vibrational excitation of $C_2H_2^+ (v_3=1,J)$ increases the rate of the title reaction by more than three orders of magnitude, while rotation hinders the reaction. The fine-structure state of the parent ion does not affect its reactivity. Ways are pointed out to apply the method to various classes of molecular ions.
 [DOI: 10.1063/1.1487373]

INTRODUCTION

Spectroscopic methods which make use of optical detection schemes such as laser absorption spectroscopy or laser induced fluorescence are generally restricted to species which can be formed in large quantities. Due to the transient nature of ions this is a formidable task for most molecular ions. Very successfully, discharges are used for obtaining high enough densities,[1] recently also in combination with the cavity ring down method.[2] However, even with a simple precursor molecule, plasma chemistry gives rise to a lot of molecular species (neutrals, ions as well as radicals) which may absorb in the spectral range of interest. Usually this leads to a spectral congestion which has to be sorted out very carefully.[1] Alternatively, various spectroscopic approaches have been based on fast ion beams and charge transfer detection schemes.[3] In most of these processes, the interaction time is very short and the dependence of the cross sections on the internal excitation of the ion is very small, especially in the case of infrared excitation. To overcome some of these problems ion trapping, guiding and swarm techniques have been combined with laser excitation. Examples include chemical probing of vibrationally excited ions in an ICR cell,[4] and laser induced charge transfer in a drift tube.[5] Well established is the method of laser induced predissociation of metastable ions or weakly bound ion complexes using an rf octopole ion guide for collecting the charged fragments.[6–8] The experiments presented in this paper are based on a 22-pole-trapping apparatus, which has been developed for studying ion–molecule reactions at low temperatures (10 K–300 K).

For LIR spectroscopy one has to select the reaction partners such that the reaction rate, relevant for the ion of interest, sufficiently changes if the ion absorbs a laser photon. In the ideal case this is a weakly endothermic reaction which is very slow in the cold environment of the trap. An excitation spectrum is recorded by iteratively detecting the product signal as a function of the laser frequency under otherwise identical conditions. A recently published example is the laser induced charge transfer (CT) $N_2^+ + h\nu + Ar \rightarrow N_2 + Ar^+$.[9] In the present study, the LIR spectroscopy is extended into the infrared regime. In particular, the method has been applied to record a ro-vibrational spectrum of the polyatomic molecular ion $C_2H_2^+$. For detecting the excitation of the acetylene ion, the reaction

$$C_2H_2^+ + H_2 \rightarrow C_2H_3^+ + H \tag{1}$$

which is very slow below 300 K, has been used.

Reaction (1) has been the subject of a variety of experimental and theoretical studies. It has been concluded from various experiments[10,11] that this reaction is endothermic by about 50 meV leading to a rate coefficient well below $10^{-12}\,cm^3/s$ at the temperatures of the present experiment (10 K–150 K). One report from a very low temperature free jet expansion experiment reveals that the reaction is exothermic.[12] Some recent experiments report the H_2 loss

TABLE I. Rates and rate coefficients at $T=90$ K relevant for the kinetics model shown in Fig. 2.

Rates/Rate coefficients	Quantity	Symbol	Value	Units	Ref.
Spectral energy density					
	Diode laser system	ρ	3.9×10^{-17}	Js/m^3	This work
	Difference frequency generation laser system	ρ	3.7×10^{-16}	Js/m^3	This work
Absorption rate					
	Diode laser system	R_{abs}	18.3	1/s	
	Difference frequency generation laser system (cw equivalent)	R_{abs}	172	1/s	
Emission rate	Einstein A coefficient	A	520	1/s	17
Rate coefficients					
	Langevin	k_L	1.59×10^{-9}	cm^3/s	
	Radiative association	k_{rad}	7×10^{-14}	cm^3/s	11
	Ternary association	k_3	7.2×10^{-26}	cm^6/s	11
	Vibrational relaxation	k_{rlx}	2×10^{-11}	cm^3/s	19
		k_{rlx}	$(1.33\pm0.04)\times10^{-9}$	cm^3/s	This work
	Reaction ($v_3=1$, $J'=8.5$)	k^*	$(2.6\pm0.4)\times10^{-10}$	cm^3/s	This work
	Reaction ($v_3=0$)	k	$<10^{-13}$	cm^3/s	10, 11
Population	Thermal population ($T=90$ K, $J''=8.5$)	g	0.025		

from $C_2H_4^+$ ions using a threshold photoelectron photoion coincidence spectrometer.[13] For the near thermoneutral reaction (1) interesting effects of the internal excitation (vibration, rotation, fine structure) can be expected.

It has been shown in a sensitive low number density experiment[11] ($10^9\,cm^{-3}$–$10^{12}\,cm^{-3}$) and corroborated by phase space calculations[14] that, at low temperatures, the dominant loss of $C_2H_2^+$ ions occurs via radiative association,

$$C_2H_2^+ + H_2 \rightarrow C_2H_4^+ + h\nu, \tag{2}$$

having a rate coefficient of only $k_r=7.1\times10^{-14}\,cm^3/s$ (80 K). Therefore almost no loss of $C_2H_2^+$ occurs and very few $C_2H_3^+$ products are formed at low temperatures without laser excitation. In summary it was expected from all these results that detection of $C_2H_3^+$ can be a sensitive monitor for $C_2H_2^+$ excitation provided reaction (1) is enhanced by the rovibrational excitation of the parent ion.

Laser induced reaction is not only a means of very sensitive spectroscopy. Since absorption of a laser photon is followed by molecular collision processes, in particular reactive collisions, LIR is an interesting tool to determine state specific rate coefficients and to learn more about the role of vibration, rotation and fine-structure states in the associated reaction dynamics. This ability has been first demonstrated for the charge transfer system $N_2^+ + Ar$.[9] In this case rate coefficients for the CT reaction and rotational inelastic collisions of vibrational ground state N_2^+ have been determined. Also upper boundary values for the probability of a fine structure change or a nuclear spin flip have been found. In the present study a simple kinetics model will be presented and used to determine rotational state specific rate coefficients for the title reaction.

After a short description of the experimental details of the trapping apparatus and the production of the IR laser light, results on the spectroscopy will be given and compared to previous experiments using a conventional absorption apparatus. Next a model kinetics system describing the well-defined elementary processes occurring in the trap will be given. Experimental results measured for various parameters are presented in the following section and rate coefficients are derived employing the results of the kinetics model. In the final section these results are discussed in the framework of the role of a $C_2H_4^+$ collision complex. The paper is concluded with an extensive discussion of future applications and possible technical extensions of this new method of LIR.

EXPERIMENT

The experimental setup is described in detail elsewhere.[15] Briefly, mass selected ions are confined in an temperature variable rf multipole trap where they can react with ambient gas. After selected storage times, primary ions as well as reaction products are extracted from the trap, mass analyzed and detected with almost unit detection efficiency using conventional ion counting.

In the present experiment, acetylene ions which are produced by electron bombardment in an ion storage source containing a (C_2H_2, H_2) gas mixture, are stored for long

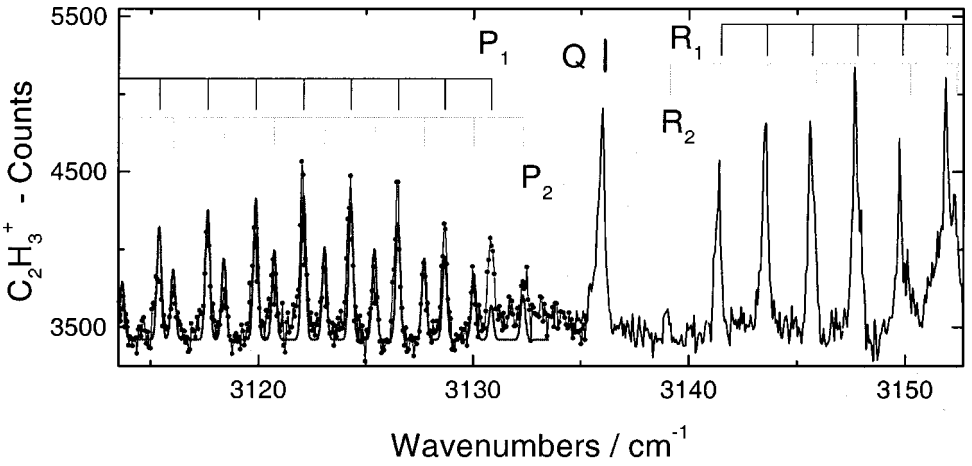

FIG. 1. Rotationally resolved LIR spectrum of the antisymmetric C–H stretching vibration of $C_2H_2^+$. $C_2H_3^+$ products are used as a monitor for the excitation of the parent ions. The positions of the *P*, *Q*, and *R* branches, calculated from high resolution laser absorption data published by Oka's group (Ref. 1), are indicated by the four scales. For the *P* branch a simulated spectrum is shown as a solid line, assuming a rotational temperature of $T=90$ K.

times in an rf 22-pole ion trap at low temperatures and various hydrogen densities. Typical parameters used for the results of this paper were a storage time of 2 s, an ambient temperature of 90 K and a target gas number density of $2.7\times10^{11}\,n\text{-}H_2\,/\text{cm}^3$. The stored ion ensemble was exposed to IR laser light at about 3140 cm^{-1} corresponding to the asymmetric C–H stretching mode (ν_3) of the acetylene ion. The IR radiation has been generated by difference frequency mixing of a Nd:YAG pumped dye laser and the fundamental of a seeded Nd:YAG. Maximum pulse energies of 2 mJ of IR radiation at a repetition rate of 30 Hz and a band width of $\Delta\nu=0.24$ cm^{-1} have been obtained. The spectral energy density experienced by the ion cloud is given by

$$\rho=P/(A_{\text{eff}}c\Delta\nu), \tag{3}$$

where P is the corresponding cw laser power and A_{eff} is the effective cross-sectional area of the laser and the ion cloud in the trap. The dimension of the latter is larger than the cross section of the laser beam inside the trap. Due to the statistical nature of the absorption process and the fact that each ion explores much of the trapping volume during a storage time of seconds it is thus safe to assume that A_{eff} is given by the cross section of the ion cloud which has been calculated previously[9] to be about 0.57 cm^2. Multiplied with the Einstein *B* coefficient this spectral intensity gives the laser excitation rate

$$R_{\text{abs}}=\rho B_{i\to f}, \tag{4}$$

which is important for the kinetics discussed below. For that purpose the spectral energy density and the laser excitation rate of the pulsed laser system are summarized in Table I. For absolute frequency calibration absorption in CH_4 was used. The linearity of the frequency scan provided by stepping the grating of the dye laser was checked with a 9.8 GHz etalon. After the storage time of 2 s during which the ion sample has been exposed to 60 laser shots, the number of $C_2H_3^+$ products were counted. For improving the S/N ratio the procedure injection, irradiation, reaction and extraction has been repeated 20 times before the laser was tuned to the next frequency.

For the kinetics studies, a diode laser system with a cw output of 0.7 mW distributed among 3 to 4 modes has also been used. The linewidth of the mode of interest has been determined as $\Delta\nu=0.01$ cm^{-1}. The spectral energy density, ρ, is about 10 times smaller than the corresponding equivalent cw value for the pulsed laser system (see Table I). Due to the fact that the product $R_{\text{abs}}(\text{peak})\Delta t_{\text{pulse}}>1$ for the pulsed laser system, the number of excited species is limited by the number of available ground state species (state *i*) in this case. This saturation effect leads to a smaller average number of excited species as compared to the equivalent cw operation. Consequences from this finding on the results of the kinetics study are discussed below.

SPECTROSCOPY

The result of a laser scan while monitoring trapped $C_2H_3^+$ reaction products is shown in Fig. 1. It exhibits the *P*, *Q*, and *R* branch of the ν_3 fundamental of $C_2H_2^+$. This spectrum clearly shows that exciting the ν_3 mode of $C_2H_2^+$ enhances the efficiency of reaction (1) substantially. Due to the limited resolution of the laser system, the *Q* branch appears unresolved. In this way it becomes one of the dominant peaks although the Hönl–London factors for these transitions are unfavorable. In the *P* branch the spin–orbit splitting is fully resolved while it is only partly resolved for the *R* branch. Each rotational line consists of two contributions due to Λ doubling which remains also unresolved with the bandwidth of the present laser system. The multiplicity of the ortho and para nuclear spin configuration of $C_2H_2^+$ is hidden in this doublet according to symmetry considerations.[1] For comparison with previous high resolution laser absorption data published by Oka's group[1] the positions of each individual ro-vibrational transition for the two fine structure components are depicted by the scales atop the present experimental spectrum. Considering the limited spectral resolution of the present study the peak positions are in very good agreement with the earlier results.

As can be seen from Fig. 1, about 1000 $C_2H_3^+$ ions are produced in addition when the laser is tuned to a favorable transition. As described above the integration time was 40 s, i.e., 20 iterations with 2 s each. This signal was obtained with about 1700 parent ions filled into the trap each time. These small numbers of initial ions demonstrate the very high sensitivity of the LIR spectroscopy. Note that a S/N ratio of better than 10 is reached with a total of only ~34 000

parent ions per wavelength step. The present background level of about 3400 $C_2H_3^+$-product ions is also present without the laser. It is mainly due to internally hot acetylene ions which have not been quenched in the ion source, partly due to an elevated kinetic energy the ions have directly after injection, and to a small fraction due to C_2HD^+ formation. The enhancement due to vibrational excitation is about 35%. This figure can be largely increased when the cooling process of the $C_2H_2^+$ ions is improved, both in the storage ion source and by using an intense He pulse for cooling the ions in the trap as described in detail in Ref. 16. With these changes of the experimental conditions it will be possible to obtain background free spectra. For a further improvement of the S/N ratio, the conversion of primary ions should be increased in future experiments. The current maximum signal level corresponds to total conversion of about 3% in 2 s, i.e., 5×10^{-4} per laser shot. Thus there is ample room for further improvement of the signal level, because in principle, all primary ions can be converted into products.

The high sensitivity of the LIR spectroscopy allows one to record high quality spectra. The Doppler broadening can be rather small since one can work at temperatures as low as 10 K, in other traps at even lower temperatures. The ion $C_2H_2^+$ has been used as a test case since good spectral constants are known for the ν_3 band from the Oka group. The present results are in good agreement with the published data. Replacing the laser used with a diode laser spectrometer a spectral resolution which is given by the low temperature Doppler width (<100 MHz) can be obtained. The method can be used to obtain accurate values for Λ doubling even for small rotational quantum numbers. With this laser, also low lying vibrations such as the antisymmetric bending vibration of $C_2H_2^+$ (Π_u bending) can be excited. This frequency is not known to spectroscopic accuracy to date. Other spectroscopic applications are possible, e.g., excitation spectra involving two IR photons. Especially when using pulsed gas inlets and pulsed lasers, as in the present experiment, pump–probe experiments on the millisecond time scale become feasible. In such experiments lifetimes of vibrational states can be determined.

KINETICS MODEL AND RESULTS

At first sight it seems to be a problem of the LIR-method to understand quantitatively the measured intensities. This can be seen in Fig. 1 where the P branch of the experimental spectrum is compared to a simulated spectrum of a $T=90\,\mathrm{K}$ ensemble of $C_2H_2^+$. For the simulation the light absorption cross sections, Hönl–London factors as well as the thermal population of the absorbing levels have been considered as in the case of absorption spectroscopy. Obviously there is a difference between the measured and calculated spectra. Lower rotational states are slightly underestimated and higher rotational states are overestimated in the simple simulation. In comparison to absorption spectroscopy here the signal is, in addition, influenced by several competing kinetic processes. These processes are described in the following set of chemical reactions which are shown schematically in Fig. 2. Rates and rate coefficients related to the individual steps are listed in Table I. The laser induced kinetics starts with the excitation of the parent ion to a particular ro-vibrational level, indicated by the bold energy level (rate: R_{abs})

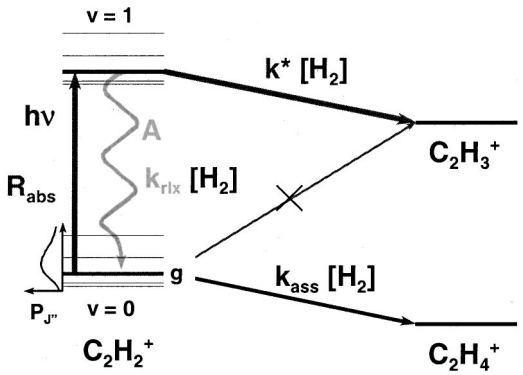

FIG. 2. Kinetics model. Reaction pathways for the formation of vibrationally excited $C_2H_2^+$, $C_2H_3^+$ products, and $C_2H_4^+$ products are given as arrows. Rates associated with these pathways are given by the corresponding symbol. Values for the rates and rate coefficients are given in Table I. They have been determined by comparing the analytical solution of the set of master equations to experimental data shown in Figs. 3 and 4.

$$C_2H_2^+(v=0,J'')+h\nu_{\mathrm{Laser}}\rightarrow C_2H_2^{+*}(v=1,J'). \tag{5}$$

Instead of reacting with an H_2 target molecule (rate coefficient: k^*)

$$C_2H_2^{+*}(v=1,J')+H_2\rightarrow C_2H_3^+ + H, \tag{6}$$

the excited ion can also fluoresce back to the vibrational ground state (Einstein A coefficient)

$$C_2H_2^{+*}(v=1,J')\rightarrow C_2H_2^+(v=0,J)+h\nu. \tag{7}$$

In this way [reactions (5)–(7)] the rotational state distribution of the ground state $C_2H_2^+$ is changed depending on the Hönl–London factors. According to an *ab initio* calculation the intensity of the ν_3 band is about 400 km/mole[17] corresponding to a lifetime of about 2 ms. At the density used in the present experiment, $[H_2]=2.7\times10^{11}\,\mathrm{cm}^{-3}$, about one collision with H_2 occurs on this time scale. Note, however, that such a collision does not necessarily lead to the formation of products as given by reaction (6) but also quenching of the vibrational excitation (k_{rlx}) can occur

$$C_2H_2^{+*}(v=1,J')+H_2\rightarrow C_2H_2^+(v=0,J'')+H_2. \tag{8}$$

In the description of the kinetics, one also has to account for the loss of primary ions by radiative (k_{rad})

$$C_2H_2^+ + H_2\rightarrow C_2H_4^+ + h\nu \tag{9}$$

and ternary association (k_3)

$$C_2H_2^+ + 2H_2\rightarrow C_2H_4^+ + H_2, \tag{10}$$

both forming $C_2H_4^+$ products. Reactions (9) and (10) are denoted as $k_{\mathrm{ass}}=k_{\mathrm{rad}}+k_3[H_2]$ in Fig. 2. In some cases also secondary reactions of the products have to be considered (not shown in Fig. 2).

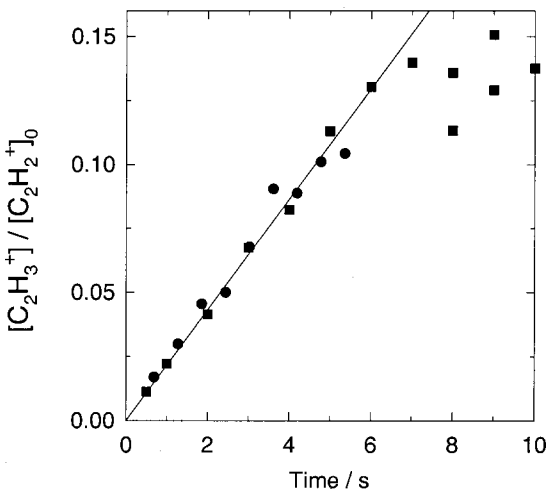

FIG. 3. Dependence of the $C_2H_3^+$ product signal on the irradiation time at a constant $[H_2]$ number density of 2.6×10^{11} cm^{-3}. Up to 6 seconds the signal increases linearly, solid line. From the slope the rate coefficient for reaction of the vibrationally excited acetylene, k^*, is determined.

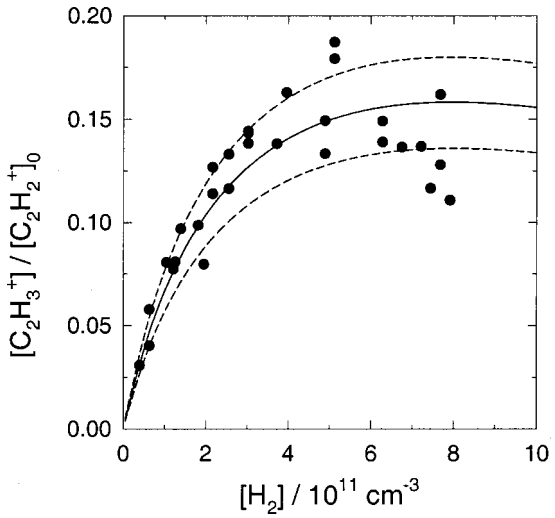

FIG. 4. Density dependence of the $C_2H_3^+$ product signal. For small $[H_2]$ number densities the signal increases linearly. A similar estimate for k^* as for the temporal dependence is derived from this behavior. The saturation effect for densities larger than 2×10^{11} cm^{-3} is explained in the text. Using the kinetics model shown in Fig. 2 values for k^* and k_{rlx} have been determined, see Table I. The solid line shows the best fit solution of the kinetics model with $k_{rlx}=1.33\times10^{-9}$ cm^3/s and $k^*=2.6\times10^{-10}$ cm^3/s. The dashed lines represent the uncertainty limit for these values as given in Table I.

Especially important is the fact that the trapping experiment deals with a finite number of stored ions. Since the laser induced reaction causes a loss of those ions which are in the particular ground state level (J'') pumped during a scan, long exposure to the laser leads to an exponential depletion of this level, if one assumes that there are no processes refilling this hole in the distribution. Note that for example the reverse reaction of reaction (6) does not take place because there is no atomic hydrogen in the trap, $[H]=0$. Inelastic collisions between remaining ions and hydrogen molecules repopulate the state the laser interacts with. For these processes different efficiencies have to be considered for the relaxation of molecular rotation, fine structure and the Λ-doublet components with opposite parity.

Figure 3 shows the normalized formation of $C_2H_3^+$ products, $[C_2H_3^+]/[C_2H_2^+]_0$, as a function of the storage time when pumping the transition $P(9)$ with the diode laser system. Up to about 6 seconds the number of product ions increases linearly with the time the ions are exposed to the laser. Up to this point more than 10% of the primary ions are converted into products. This quantity largely exceeds the 2.5% which is calculated from the thermal population of the ground state level which is pumped. This result shows that rotational relaxation is happening on a time scale shorter than seconds, i.e., in fewer than 400 collisions. Therefore it is safe to assume for our analysis that $C_2H_2^+(J'')$ and $C_2H_2^+(J\neq J'')$ are in thermal equilibrium at any time

$$[C_2H_2^+(J'')]/[C_2H_2^+]=g=[C_2H_2^+(J'')]_T/[C_2H_2^+]_T = \text{const}, \tag{11}$$

where g is the thermal population of state J'' (see Table I) and the subscript T refers to a thermal equilibrium distribution. In our model the two fine structure states are also thermally populated. Due to the stepwise scheme represented by the kinetics diagram given in Fig. 2, a very simple expression for the number of product ions can be derived

$$[C_2H_3^+]/[C_2H_2^+]_0=k_1/k_2[1-\exp(-k_2[H_2]t)] \tag{12}$$

with the sequential rate coefficient, k_1, for forming $C_2H_3^+$ products

$$k_1=k^*gR_{abs}/(A+k_{rlx}[H_2]+k^*[H_2]) \tag{13}$$

and with the rate coefficient for loss of primary acetylene ions

$$k_2=k_1+(k_{rad}+k_3[H_2]). \tag{14}$$

In the linear regime of the temporal evolution of products shown in Fig. 3 the effective rate of products is

$$K_t=\Delta[C_2H_3^+]/[C_2H_2^+]_0/\Delta t = k^*[H_2]gR_{abs}/(A+k_{rlx}[H_2]+k^*[H_2]). \tag{15}$$

Solving this equation for k^* yields

$$k^*=K_t(A+k_{rlx}[H_2]+k^*[H_2])/([H_2]gR_{abs}). \tag{16}$$

Since the Einstein A coefficient is larger than $k_{rlx}[H_2]$ or $k^*[H_2]$ as will be shown below, k^* can be calculated without a precise knowledge of k_{rlx}. The result for k^* is 1.1×10^{-10} cm^3/s for this particular rotational state in the limit $A\gg k_{rlx}[H_2]+k^*[H_2]$. Assuming as an upper limit for $k_{rlx}[H_2]+k^*[H_2]=k_L^*[H_2]$, where k_L is the collision limit (see Table I), the upper limit for k^* in this approximation is 2.0×10^{-10} cm^3/s. It can be seen from the scatter in Fig. 3 that the error in the slope is about $\pm20\%$. For times larger than about 6 seconds the increase in products levels off significantly. This finding is due to the finite number of trapped ions which, according to the kinetics diagram, finally end up either as $C_2H_3^+$ or $C_2H_4^+$ products. Therefore the maximum number of product ions is limited by the number of parent ions.

The same effect can be seen when studying the number of $C_2H_3^+$ product ions as a function of the H_2 number density. A typical result of such a measurement is shown in Fig. 4 for the same transition, $P(9)$, as pumped during the temporal evolution in Fig. 3. The storage time is kept constant, $t=4$ s, for all these measurements. For small $[H_2]$ number densities the number of products increases linearly. For densities larger than $(2-3)\times10^{11}\,\mathrm{cm}^{-3}$ the yield levels off and for densities larger $10^{12}\,\mathrm{cm}^{-3}$ the yield tends to fall even below that level (not shown in Fig. 4). As for the temporal evolution the linear regime can be used to determine the rate coefficient k^*. In analogy to Eq. (15) the slope K_n, where the subscript n refers to the density, is given by

$$K_n=[C_2H_3^+]/[C_2H_2^+]_0/[H_2]$$
$$=k^*\Delta t g R_{\mathrm{abs}}/(A+k_{\mathrm{rlx}}[H_2]+k^*[H_2]). \quad (17)$$

In the low density limit, $A\gg k_{\mathrm{rlx}}[H_2]+k^*[H_2]$, Eq. (17) can be simplified and solved for k^*,

$$k^*=K_nA/(\Delta t g R_{\mathrm{abs}}). \quad (18)$$

In this limit k^* is estimated to be about $1.6\times10^{-10}\,\mathrm{cm}^3/\mathrm{s}$. Taking the finite value for $k_{\mathrm{rlx}}[H_2+k^*[H_2]$ again into account one arrives at $2.9\times10^{-10}\,\mathrm{cm}^3/\mathrm{s}$ when using the low density slope given in Fig. 4. This value has a larger uncertainty than the estimate using the temporal evolution of products due to a larger scatter in the data points and due to the limited linear regime. However, within these limitations both estimates, temporal evolution and density dependence, agree reasonably well around $2\times10^{-10}\,\mathrm{cm}^3/\mathrm{s}$. Several conclusions on the size of the other rates and rate coefficients can be drawn from these results. Their impact on the interpretation of the $C_2H_2^{+*}(v=1,J')+H_2$ collision will be discussed in the following section.

DISCUSSION

The linear range of product formation has been used to derive reliable values for the rate coefficient of the reaction of vibrationally and rotationally excited acetylene ions. Next, reasons for the saturation effects seen in Figs. 3 and 4 will be discussed. Whereas

$$A\gg k_{\mathrm{rlx}}[H_2]+k^*[H_2] \quad (19)$$

was an assumption to simplify Eq. (17), this relation must hold for the linear regime of the density dependence. In the opposite case the number of products, $[C_2H_3^+]/[C_2H_2^+]_0$, would be independent of $[H_2]$ as can be easily seen from Eq. (17). From this finding it can be concluded that the vibrational relaxation, $k_{\mathrm{rlx}}[H_2]$, as well as the reaction, $k^*[H_2]$, must be slower than the Einstein A coefficient for densities $[H_2]<2\times10^{11}\,\mathrm{cm}^{-3}$. Taking the estimated value for k^* and the Einstein A coefficient of Table I inequality (19) holds. In return the upper limit of the $[H_2]$ density can be derived for which a saturation in the density dependence is expected. Assuming $k_{\mathrm{rlx}}\ll k^*$ when comparing the only other value for k_{rlx} of excited $C_2H_2^+$ from a trap experiment (see Table I) to k^* from our first analysis, this limit should be about $2.5\times10^{12}\,\mathrm{cm}^{-3}$. This is far above the value where deviations from the linear response are observed in the present study. Using a similar argument nonlinear terms in the temporal evolution should not appear on the time scale shown in Fig. 3. Therefore saturation of the product signal is not occurring due to competition of fluorescence and reaction but rather due to the competition of association and reaction and/or relaxation and reaction. The influence of association (included in k_2) can be seen when taking the second order term in time in Eq. (12) into account which has been neglected in Eq. (15),

$$[C_2H_3^+]/[C_2H_2^+]_0=k_1[H_2]t-1/2k_1k_2[H_2]^2t^2+\mathrm{O}(t^3). \quad (20)$$

In order to incorporate the more complete kinetics indicated in Fig. 2 in the analysis of the density dependence, a set of four differential equations involving ground state acetylene, the vibrationally excited species, the association products and the protonated acetylene product

$$d/dt[C_2H_2^+]=(-gR_{\mathrm{abs}}-(k_{\mathrm{rad}}[H_2]+k_3[H_2]^2))[C_2H_2^+]$$
$$+(A+k_{\mathrm{rlx}}[H_2])[C_2H_2^+]^*, \quad (21)$$

$$d/dt[C_2H_2^+]^*=+gR_{\mathrm{abs}}[C_2H_2^+]-(A+k_{\mathrm{rlx}}[H_2]$$
$$+k^*[H_2])[C_2H_2^+]^*, \quad (22)$$

$$d/dt[C_2H_3^+]=+k^*[H_2][C_2H_2^+]^*, \quad (23)$$

$$d/dt[C_2H_4^+]=+(k_{\mathrm{rad}}[H_2]+k_3[H_2]^2)[C_2H_2^+] \quad (24)$$

has been solved analytically. The solution for $[C_2H_3^+]$ has been used to simulate the behavior found in Fig. 4. The result of the solid line curve shown in this figure is given in Table I. The dashed lines correspond to the error margins also given in Table I. In the fit procedure k^* and k_{rlx} have been let free. The rates for absorption and fluorescence have been held fixed in accordance with the assumption made for the linear regime above. Rate coefficients for association have been determined in a separate experiment without laser but their influence on the number of $C_2H_3^+$ products has been checked in the simulation too.

With this simple fit procedure similar values for k^* are obtained as in the first analysis, since the linear increase sensitively depends on this quantity. Of course other quantities related to the laser excitation and fluorescence play an equally important role for the number of products, as could be seen already in Eq. (15). Interestingly this figure only depends on the ratio of the Einstein A and B coefficients. Therefore the outcome does not strongly depend on the dipole matrix element for the transition but rather on the spectral energy density of the laser light. This makes the results robust against uncertainties of the calculated IR band intensities.[17] The intensity of the laser light has an error margin of roughly 30%–40% taking into account the uncertainties of the overlap of the ion cloud and the laser beam or the distribution of the laser power among the three to four modes of the laser. This error and the error in determining the absolute $[H_2]$ number density are the major sources of error for k^*. Despite these deficiencies k^* is determined within a factor of 2. In Table I only the statistical error found in the fit

procedure is given. In order to compare this rate coefficient to the Langevin limit the rotational dependent values will be presented below.

Concerning the saturation effects the simulation shows that the saturation level is very sensitive to changes in the rate coefficients for the association reaction as well as to changes in the one for relaxation. This is due to the fact that the rate to form $C_2H_3^+$ products is directly reduced by the association reaction. In the simulation it has been found that an increased value of the association rate coefficient would lead even to a reduced number of products for higher densities. Relaxation, however, leads to a substantial decrease of $C_2H_3^+$ products only when $k_{\mathrm{rlx}}[H_2]$ reaches the order of magnitude of A, see Eq. (19). Since there is no other free parameter in our model the only way of explanation of the saturation effect is a large value for the rate coefficient of relaxation, k_{rlx}, see Table I and the simulation in Fig. 4.

As the $C_2H_2^+(v=1)+H_2$ collision is considered to be without a barrier in the entrance channel, a $C_2H_4^+$ complex will be formed at collision rate, k_L. From this complex three outcomes are possible, (i) reaction, (ii) pure rotational relaxation which still leaves enough energy in the $C_2H_2^+$ reactant to form $C_2H_3^+$ products in the next collision, and (iii) vibrational–rotational relaxation. Outcome (ii) is not distinguishable from (i) in the trap experiment and thus contributes to k^*. Vibrational–rotational relaxation (iii) does not necessarily lead to vibrational ground state $C_2H_2^+$. However, since the energy of the lowest lying vibration of $C_2H_2^+$ exceeds the endothermicity of the reaction, process (iii) and the corresponding rate coefficient k_{rlx} is related to the formation of vibrational ground state $C_2H_2^+$. With these assumptions the sum of k^* and k_{rlx} adds up to k_L. Since $k^*<k_L$, as seen in this study, the rate coefficient k_{rlx} can be expected to be of the order of the collision rate, k_L. In the simulation shown in Fig. 4 we find k_{rlx} between $0.81k_L$ and $0.87k_L$ (dashed line) which is indeed a substantial fraction of the Langevin rate. This result is indicative that the complex formation is happening without dynamical restriction. A similar behavior has been seen for the competition of rotational vs vibrational–rotational relaxation of excited OH/OD($A\,^2\Sigma$) in collisions with Ar.[18]

Unfortunately no other measurements of the relaxation rate coefficient for $C_2H_2^+ + H_2$ collisions are available at present. Relaxation processes for $C_2H_2^+ + CH_4$ in a 22-pole trap experiment reveal a rather small rate coefficient of $2\times10^{-11}\,\mathrm{cm^3/s}$.[19] Since these studies were performed on the thermal (300 K–400 K) distribution of ions from a storage ion source, bending modes are much more likely to be excited and quenched in that study than the ν_3 stretching vibration which has been selectively excited in this work.

Using the difference frequency laser system kinetics studies could be made as a function of the rotational quantum number of the ground state acetylene ion. H_2 densities and storage times in these experiments were chosen in the linear regime, $[H_2]<3\times10^{11}\,\mathrm{cm^{-3}}$ and $t=2$ s, in order to assure a linear response of the number of $C_2H_3^+$ product ions. As has been pointed out above in the spectrum a maximum of 3% of the primary ions is converted to $C_2H_3^+$ products. Therefore also the brighter, pulsed laser source does not give rise to the saturation effect which has been described above. In view of the high spectral laser intensity this finding seems surprising. A closer inspection of the pulsed excitation process reveals that in the current limit, $R_{\mathrm{abs}}(\mathrm{peak})\Delta t_{\mathrm{pulse}}>1$, the number of excited ions is restricted by the number of ground state parent ions rather than by the corresponding cw-excitation rate, $R_{\mathrm{abs}}(\mathrm{cw})$, see Table I. Therefore the reaction rates for the two different laser systems are not as different as expected from the spectral energy densities.

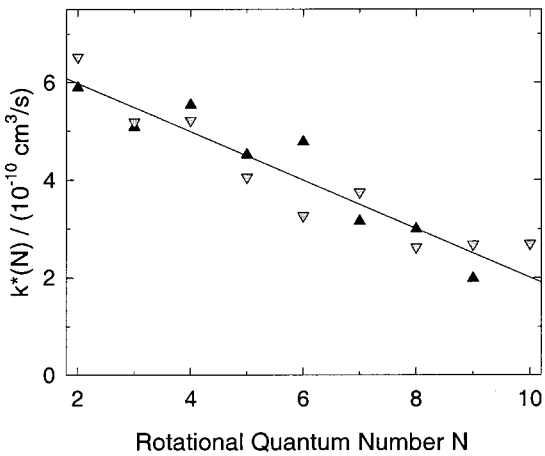

FIG. 5. State specific rate coefficient for reaction (1), k^*, as a function of the rotational state of the primary ion. Values for the two fine-structure states (▲: F_1, ▼: F_2) show a similar decrease for higher rotational excitation.

With these remarks the difference between the observed spectrum and the simulated spectrum shown in Fig. 1 is due to the dependence of the rate coefficient, k^*, on the rotational state of the vibrationally excited acetylene ion. This dependence is shown in Fig. 5. The absolute value is calibrated via the measurements on the $P(9)$ transition using the diode laser system. The apparent rate coefficient drops by 50% when going from $N''=2$ to $N''=10$. To date it is not clear what are the reasons for this rotational dependence. In view of the model discussed to explain the low density saturation effect, the rotational dependence of k^* might indeed be a rotational dependence of k_{rlx} which—in this model—appears in k^* via the relation

$$k^*(J')=k_L-k_{\mathrm{rlx}}(J'). \tag{25}$$

In fact it seems very likely that the rate for vibrational relaxation increases with the rotational quantum number as the number of energetically accessible states increases accordingly.

Another interesting result of Fig. 5 is that the rate coefficient does not seem to depend on the fine-structure state of the primary ion since both subsets fall on the same line. Finally one can conclude that a substantial fraction of the collisions lead to reaction since the rate coefficient amounts to about 16% of the Langevin limit and for small rotational quantum numbers even to about 40%, see Fig. 5 and Table I.

All the results, especially the spectra and thus the rotational dependence of k^* have been reproduced many times. However, careful further checks on the signal dependence including the laser power, etc., have to be carried out. In summary the results show that state specific preparation of

ions with the use of chemical probing as a monitor, i.e., laser induced reaction, can reveal details on the dynamics of the collision system. However, theoretical support is needed to link the experimental results to details of the potential energy surface, e.g., its anisotropy and possible coupling of states in the entrance channel.

FUTURE PERSPECTIVES OF LASER INDUCED REACTIONS

With its very high sensitivity and the possibility of obtaining background free spectra of mass analyzed species it is interesting to apply LIR spectroscopy to other ions, i.e., other reaction systems. In a more general scheme the reactions and therefore the ions involved have to fulfill the following requirements: (i) there must be a bimolecular reaction which is slightly hindered (barrier or endothermicity), (ii) if there are competitive reaction channels they must be slow, and (iii) the reactivity must be enhanced by the laser excitation. At first sight this seems to restrict the number of possible candidates substantially. However, there is a whole class of reactions including hydrocarbons, which are comparable to the present system, e.g., $C_3H^+ + H_2$.[20] A second class of reactions involves proton transfer as a way of chemically probing the excitation of the parent ion. There is a third, huge class of reactions which are perfectly suited for low temperature studies: isotopic fractionation. Due to the difference in zero point energy isotope exchange reactions are always hindered in one direction. Therefore laser induced inhibition of isotope enrichment can serve as the spectroscopic signal.

Finally, instead of looking for unimolecular[6] or bimolecular reactions,[9] a sensitive thermodynamic equilibrium can be utilized for probing the laser excitation. With traps it is possible to establish a low temperature chemical equilibrium which is then altered upon laser excitation of one species. For example, when storing H_3^+ in the presence of H_2, the natural abundance of HD in H_2 will lead to a large H_2D^+/H_3^+ ratio. This ratio is very sensitive to heating or cooling the ensemble as can be seen from the large differences in composition when using parahydrogen instead of normal hydrogen. As a consequence LIR can lead to a dramatic perturbation serving as a very sensitive spectroscopic probe of parent as well as daughter ions.

ACKNOWLEDGMENTS

The authors are very grateful to Dr. T. Glenewinkel-Meyer and U. Gerken for the assistance with the laser system. This work was in part funded by the DFG in the Schwerpunktprogramm SPP 471/SCHL341/2-3 and by the TMR Network on Astrochemistry.

[1] M. Jagod, M. Rösslein, C. M. Gabrys, B. D. Rehfuss, F. Scappini, M. W. Crofton, and T. Oka, J. Chem. Phys. **97**, 7111 (1992); M. W. Crofton, M. Jagod, B. D. Rehfuss, and T. Oka, *ibid.* **86**, 3755 (1987).
[2] D. Pfluger, T. Motylewski, H. Linnartz, W. E. Sinclair, and J. P. Maier, Chem. Phys. Lett. **329**, 29 (2000).
[3] J.-T. Shy, J. W. Farley, and W. H. Wing, Phys. Rev. A **24**, 1146 (1981).
[4] R. Marx, G. Mauclaire, and R. Derai, Int. J. Mass Spectrom. Ion Phys. **47**, 155 (1983).
[5] M. J. Frost, S. Kato, V. M. Bierbaum, and S. R. Leone, J. Chem. Phys. **100**, 6359 (1994).
[6] D. W. Boo, Z. F. Liu, A. G. Suits, J. S. Tse, and Y. T. Lee, Science **269**, 57 (1995).
[7] S. A. Nizkorodov, O. Dopfer, T. Ruchti, M. Meuwly, J. P. Maier, and E. J. Bieske, J. Phys. Chem. **99**, 17118 (1995).
[8] S. W. Bustamente, M. Okumura, D. Gerlich, H. S. Kwok, L. R. Carlson, and Y. T. Lee, J. Chem. Phys. **86**, 508 (1987).
[9] S. Schlemmer, T. Kuhn, E. Lescop, and D. Gerlich, Int. J. Mass Spectrom. Ion Processes **185–187**, 589 (1999).
[10] D. Gerlich, in *Molecules and Grains in Space*, edited by I. Nenner (AIP Press, New York, 1994), p. 489.
[11] D. Gerlich, J. Chem. Soc., Faraday Trans. **89**, 2199 (1993).
[12] M. Hawley and M. A. Smith, J. Chem. Phys. **96**, 1121 (1992); see also discussion in J. Chem. Soc., Faraday Trans. **89**, 2209 (1993).
[13] M. Malow, F. Güthe, and K.-M. Weitzel, Phys. Chem. Chem. Phys. **1**, 1425 (1999).
[14] S. A. Malunendes, A. D. McLean, and E. Herbst, Chem. Phys. Lett. **217**, 571 (1994).
[15] D. Gerlich, Phys. Scr., T **T59**, 256 (1995).
[16] W. Paul and D. Gerlich, Proceedings of the XVIII ICPEAC Conference, Aarhus, 1993.
[17] T. J. Lee and H. F. Schaefer, J. Chem. Phys. **85**, 3437 (1986); T. J. Lee, J. E. Rice, and H. F. Schaefer, *ibid.* **86**, 3051 (1987).
[18] M. M. Ahern and M. A. Smith, J. Chem. Phys. **110**, 8555 (1999).
[19] Y. Chiu, B. Yang, H. Fu, S. L. Anderson, M. Schweizer, and D. Gerlich, J. Chem. Phys. **96**, 5781 (1992); S. Mark, Ph.D. thesis, TU-Chemnitz, 1996.
[20] A. Sorgenfrei and D. Gerlich, in *Molecules and Grains in Space*, edited by I. Nenner (AIP Press, New York, 1994), p. 505.